







RESEARCH ARTICLE | APRIL 04 2025

Phase transitions of β -ZnTe(en)_{0.5} under hydrostatic pressure

F

Julianne C. Miller ; Yizhou Wang ; Yong Zhang ; Thomas A. Schmedake 
Matthew D. McCluskey  *AIP Advances* 15, 045308 (2025)<https://doi.org/10.1063/5.0266352>View
OnlineExport
Citation**Articles You May Be Interested In**

Structural and luminescent properties of ZnTe film grown on silicon by metalorganic chemical vapor deposition

J. Vac. Sci. Technol. A (November 2002)

Unveiling the influence of ZnTe and Te layers as part of the back-contact on CdTe solar cells performance

AIP Advances (March 2021)

Molecular dynamics simulations on the local order of liquid and amorphous ZnTe

J. Chem. Phys. (May 2008)**AIP Advances****Why Publish With Us?****19 DAYS**
average time
to 1st decision**500+ VIEWS**
per article (average)**INCLUSIVE**
scope[Learn More](#)

Phase transitions of β -ZnTe(en)_{0.5} under hydrostatic pressure

Cite as: AIP Advances 15, 045308 (2025); doi: 10.1063/5.0266352

Submitted: 27 February 2025 • Accepted: 19 March 2025 •

Published Online: 4 April 2025



View Online



Export Citation



CrossMark

Julianne C. Miller,¹  Yizhou Wang,²  Yong Zhang,²  Thomas A. Schmedake,³ 
and Matthew D. McCluskey^{1,a)} 

AFFILIATIONS

¹Department of Physics and Astronomy, Washington State University, Pullman, Washington 99164-2814, USA

²Electrical and Computer Engineering Department, The University of North Carolina at Charlotte, Charlotte, North Carolina 28223-0001, USA

³Chemistry Department, The University of North Carolina at Charlotte, Charlotte, North Carolina 28223-0001, USA

^{a)}Author to whom correspondence should be addressed: mattmcc@wsu.edu

ABSTRACT

Organic–inorganic hybrid semiconductors have enhanced and distinctive material properties. β -ZnTe(en)_{0.5}, which consists of alternating layers of two-monolayer-thick zinc telluride (ZnTe) and ethylenediamine (en), exhibits high crystallinity, stability, and tunable optical properties. Using x-ray diffraction (XRD) and Fourier transform infrared spectroscopy, this study investigated the structural response of β -ZnTe(en)_{0.5} to applied hydrostatic pressure. Pressure-induced phase transitions were observed at 2.1 and 3.3 GPa. Shifts in the XRD peaks indicate substantial anisotropy in the pressure response, with the layer stacking direction (*b* axis) exhibiting high compressibility. The *a* and *b* lattice parameters showed -0.55% strain/GPa and -2.26% strain/GPa, respectively, contradicting theoretical calculations that predicted a more isotropic response. IR spectroscopy revealed abrupt changes in NH₂ and CH₂ vibrational modes corresponding to the phase transitions.

© 2025 Author(s). All article content, except where otherwise noted, is licensed under a Creative Commons Attribution (CC BY) license (<https://creativecommons.org/licenses/by/4.0/>). <https://doi.org/10.1063/5.0266352>

INTRODUCTION

Organic–inorganic hybrid semiconductors are of considerable interest due to their high solar cell efficiency¹ and applications to light-emitting diodes (LEDs).² They combine the flexibility of organic materials with the desirable electronic properties of inorganic materials.³ The II–IV organic–inorganic hybrid semiconductor β -ZnTe(en)_{0.5} has been a subject of recent attention because of its superior structural order and longer stability than most hybrid semiconductors.⁴ The incorporation of the organic layer allows for tunable optical properties,⁵ modifications to the band structure, and an increased exciton binding energy.⁶ β -ZnTe(en)_{0.5} consists of alternating layers of two-monolayer-thick ZnTe and ethylenediamine (en=C₂N₂H₈). It has both long and short-range order because the organic layers maintain their distinct configurations, and the organic layer cannot diffuse into the inorganic layer.⁷ This material has nearly as good crystallinity as simple semiconductors.^{4,7} ZnTe(en)_{0.5} may be preferable over less-ordered hybrid materials, such as MAPbI₃,⁸ for applications involving quantum coherence due

to its higher crystallinity, which could enhance electronic conductivity.⁹ In addition, some phase-change materials can be used for memory applications;¹⁰ however, these materials will often degrade over time, causing the device to malfunction.¹¹

At room temperature and ambient pressure, β -ZnTe(en)_{0.5} has an orthorhombic structure, space group P_{nmm} ,⁴ with lattice parameters $a = 5.660$ Å, $b = 17.156$ Å, and $c = 4.336$ Å (Fig. 1).¹² The en chains, typically as a solvent, have high degrees of freedom,¹³ meaning that it is expected that the *b* lattice parameter shortens more than the *a* and *c* parameters under pressure. Previous single-crystal x-ray diffraction (XRD) measurements showed that the sample has sharp, intense (0, 2*n*, 0) diffraction peaks.⁴ β -ZnTe(en)_{0.5} has also been characterized by EDX, SEM, XPS, and a range of optical and electrical methods.⁴ Hydrostatic pressure has been used widely to study the material properties of semiconductors.¹⁴ However, studies on anisotropic systems, particularly organic–inorganic hybrid structures, are rare. By examining the pressure response of β -ZnTe(en)_{0.5}, we aim to provide insight into the mechanical properties and anisotropy of the layer-stacking structure.

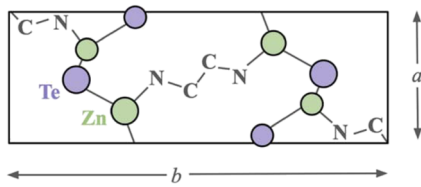


FIG. 1. Unit cell of β -ZnTe(en)_{0.5} with the *c* axis perpendicular to the page. Hydrogen atoms are not shown.

In this paper, we present evidence of pressure-induced phase transitions of β -ZnTe(en)_{0.5} at 2.1 and 3.3 GPa, obtained from x-ray diffraction (XRD) experiments performed on β -ZnTe(en)_{0.5} powder. The phase transitions observed in XRD were verified with Fourier transform infrared (FTIR) spectroscopy. Both results suggest that the organic layer is especially affected by pressure. We refer to the phases as the low-pressure phase, the second phase, and the third phase.

EXPERIMENTAL METHODS

Orthorhombic β -ZnTe(en)_{0.5} was synthesized using the procedures detailed in Refs. 4 and 5. Samples were loaded into a piston-cylinder diamond-anvil cell (DAC) along with ruby microspheres for pressure measurements. The pressures were determined using the Ruby2020 calibration¹⁵ and by averaging pressures obtained from the R_1 and R_2 lines before and after measurements. The estimated precision is ± 0.1 GPa. Stainless-steel gaskets were preindented to thicknesses of ~ 20 or $50 \mu\text{m}$ to accommodate $600 \mu\text{m}$ or 1.1 mm cutlet diamonds, respectively. For the $600 \mu\text{m}$ cutlet diamonds, a $300 \mu\text{m}$ diameter hole was drilled in the center of the indent. For the 1.1 mm diamonds, a $700 \mu\text{m}$ diameter hole was drilled.

Single crystalline β -ZnTe(en)_{0.5} plates of several hundred μm in lateral dimensions and $\sim 10 \mu\text{m}$ in thickness were loaded into the DAC for FTIR measurements. For XRD measurements, a needle was used to break the sample up into smaller pieces (grain sizes of a few μm) after being placed in the gasket hole. Three pressure-transmitting media were used: mineral oil, liquid nitrogen, and a 4:1 methanol-ethanol mixture. Mineral oil is hydrostatic up to 2.5 GPa,¹⁶ liquid nitrogen up to 24 GPa,¹⁷ and the 4:1 methanol-ethanol mixture up to 10.5 GPa.^{18,19}

The XRD experiment was carried out in a Xeuss 3.0 SAXS/WAXS laboratory beamline with a molybdenum x-ray source (0.711 \AA). The instrument, combined with the small opening of the DAC, limited the maximum scattering angle to 12° . The (011) XRD peak is predicted to be observed at $\sim 9.7^\circ$, but this peak was weak and not detected. To obtain a sufficient XRD intensity, 1.1 mm cutlet diamonds were used. Mineral oil and the 4:1 methanol-ethanol mixture were the pressure-transmitting media for low-pressure and high-pressure measurements, respectively. All spectra were recorded at ambient temperature. A measurement of lanthanum hexaboride in a diamond anvil cell at 0 GPa was used as a calibration for XRD data.²⁰ IR measurements were performed with a Bomem DA8 vacuum FTIR spectrometer using a SiC source, KBr beam splitter, and InSb detector. Spectra were taken with a resolution of 4 cm^{-1} . The

data presented in this paper were collected as pressure was increased. No evidence of hysteresis was observed (supplementary material).

RESULTS

Phase transitions

Three distinct peaks were observed in the XRD plots. Selection rules for the orthorhombic P_{mmm} space group dictate that the sum ($h + k + l$) of the Miller indices for all planes seen in the x-ray spectra must be either even-numbered or odd-numbered.²¹ The lowest scattering angle peak was assigned to the (020) reflection, while the two remaining peaks were attributed to (110) and (130). Fitting was performed on the three peaks, and the optimal *a* and *b* lattice parameters were determined. The results rule out many possibilities of non-orthorhombic structures for the higher-pressure phases; therefore, we assumed them to be orthorhombic.

The lower half of Fig. 2 shows XRD spectra for β -ZnTe(en)_{0.5} at 1.2, 1.4, and 2.2 GPa. The (130) peak is observed as a doublet, which can be attributed to the $K\alpha_1$ (0.7093 \AA)²² and $K\alpha_2$ (0.7136 \AA)²³ emission lines from the x-ray source. At lower scattering angles, the two emission lines are not resolved.

The splitting of the (020) peak at 2.2 GPa indicates a phase transition, with the higher-angle component corresponding to the second phase. The large increase in scattering angle indicates a discontinuous drop in the *b* lattice parameter. Similarly, the splitting of the (130) peak coincides with the phase change. The higher-angle component actually yields a small discontinuous increase in the *a* lattice parameter because the shift reflects the combined effect of the changes in *a* and *b*. The upper half of Fig. 2 shows XRD spectra for ZnTe(en)_{0.5} at 2.9, 3.5, and 5.2 GPa. At 2.9 GPa, the single (020) peak is evidence that the material is no longer in a two-phase region and consists of the second phase only. At 3.5 GPa, the (020) peak has split by a significant amount, indicating a mixture between the second and third phases.

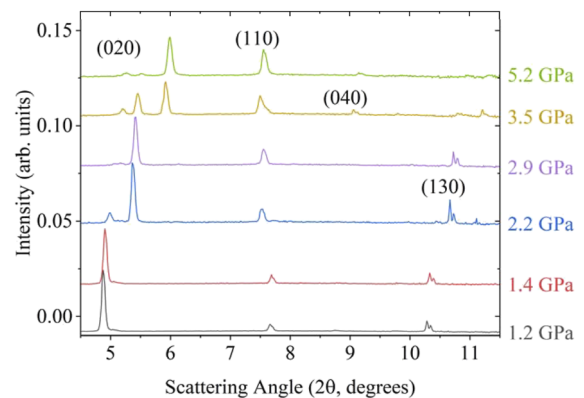


FIG. 2. XRD measurements for β -ZnTe(en)_{0.5} at six different pressures. The 1.2 and 1.4 GPa spectra show that the sample is in the low-pressure phase. The 2.2 GPa spectrum shows that the sample is in a mixed phase region, indicated by the splitting of the (020) and (130) peaks. For the 2.9 GPa spectrum, the sample is in the second phase. The 3.5 and 5.2 GPa spectra show that the sample is in a mixed phase region, indicated by the splitting of the (020) peak.

Figure 3 shows the lattice parameters from 0 to 5.2 GPa. Before the phase change, the b lattice parameter decreases rapidly, whereas the a lattice parameter exhibits minimal change. Evidently, the pressure response is highly anisotropic. At 2.1 GPa we find that the b lattice parameter in the second phase drops by $\sim 6.8\%$ while the a lattice parameter increases by $\sim 3.6\%$ relative to the first phase. These results indicate that the organic-inorganic layers become more densely packed under pressure, and more so following the phase transition. The next phase transition occurs at 3.3 GPa, where the b lattice parameter dropped by $\sim 8.8\%$ and the a lattice parameter increased by $\sim 3.2\%$.

The en molecule has two primary conformations, known as TTT and GTG', in the II-VI hybrids.²⁴ For the ZnTe-based hybrids in either the α_I or β phase, en takes the TTT conformation. In another phase that has only slightly higher energy, α_{II} , en is in the GTG' conformation, resulting in a significantly shorter lattice parameter along the stacking direction (by 3.5%). We speculate that the first phase transition could be the TTT-to-GTG' conformation change under pressure. Interestingly, this implies that the β -like high-pressure phases (with even smaller lattice parameters than those of the α phases) may have the GTG' conformation. More detailed structural studies are needed to verify this possibility.

Notably, these transitions occur at pressures significantly lower than the lowest reported pressure-induced phase change of pure ZnTe, which is 19.2 GPa.²⁵ At this phase change, pure cubic ZnTe undergoes a 6.1% volume collapse.²⁵ In contrast, the incorporation of the organic (en) layer in β -ZnTe(en)_{0.5} results in phase changes at significantly lower pressures and with more substantial decreases in the largest lattice parameter compared to pure ZnTe.

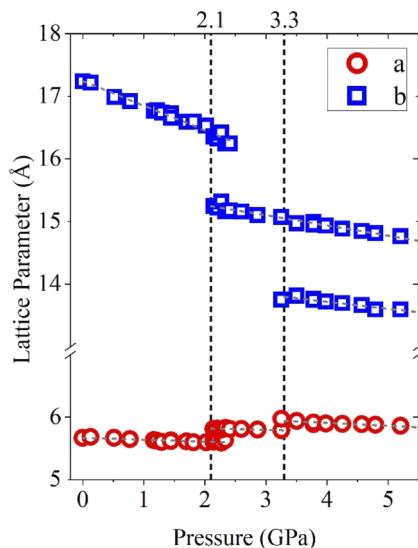


FIG. 3. Lattice parameters of β -ZnTe(en)_{0.5} as a function of pressure. Dashed lines represent linear regression fits. Two values for the lattice parameters near 2.1 GPa indicate a mixed phase. Similarly, two values for the b lattice parameter at 3.3–5 GPa indicate a mixture of the second and third phases.

Lattice parameters vs pressure

Our measured value for the a lattice parameter at 0 GPa is 5.666 ± 0.013 Å, which is consistent with the previously reported value of 5.660 Å.¹² The decrease of the a parameter is given by -0.031 ± 0.006 Å/GPa (-0.55% strain/GPa), -0.023 ± 0.008 , and -0.05 ± 0.01 Å/GPa for the low-pressure phase, second phase, and third phase, respectively. These small slopes indicate that the (100) planes experience very little compression while in a given phase, even though they are affected by the phase transitions.

The b lattice parameter at 0 GPa is 17.238 ± 0.03 Å, comparable to the previously reported value of 17.156 Å.¹² The b parameter displays significant slopes: -0.39 ± 0.02 Å/GPa (-2.26% strain/GPa) for the low-pressure phase, -0.16 ± 0.01 Å/GPa for the second phase, and -0.11 ± 0.02 Å/GPa for the third phase. The larger-magnitude slopes are consistent with the organic (en) layer being more compliant than the inorganic ZnTe layer. We note that the (010) crystal direction is the most compliant when the material is in the low-pressure phase and the stiffest when the material is in the third phase.

The significantly larger pressure coefficient along the b axis is consistent with the intuition that along the stacking direction, the structure is the most compressive. However, our results are inconsistent with the predicted elastic constants for the low-pressure phase using density functional theory (DFT) and molecular dynamics (MD).²⁶ From that theoretical work, we calculated the strain coefficients to be -1.81 (-1.41%) strain/GPa with DFT (MD) for the a axis and -1.54 (-1.66%) strain/GPa for the b axis (supplementary material). Counterintuitively, these calculated coefficients imply that the structure is *less* compressive along the stacking direction (b) than the a direction. Furthermore, the values show significantly smaller anisotropy than our observations (-0.55% strain/GPa for a , -2.26% strain/GPa for b).

IR spectroscopy

To complement the XRD experiments, FTIR spectroscopy was employed to investigate vibrational modes associated with the phase transitions. We completed measurements with two pressure-transmitting media, mineral oil and liquid nitrogen. With mineral oil, we achieved pressures as low as 0.3 GPa, which enabled an examination of the first phase transition with greater precision. With liquid nitrogen, we loaded the sample to just below the first phase transition, 1.9 GPa. It has previously been observed that en has several IR-active CH₂ and NH₂ stretching modes in the 2500–3400 cm⁻¹ range.^{27–29} We examined modes in the 3120–3300 cm⁻¹ range for measurements performed with mineral oil and modes in the 2900–3025 cm⁻¹ range for measurements performed with liquid nitrogen.

IR spectra for measurements performed with mineral oil are presented in Fig. 4. For pressures between 0.3 and 1.8 GPa, the spectra were almost identical, with a broad absorption peak at 3200 cm⁻¹, which we assigned to an NH₂ stretching vibrational mode.²⁷ Significant changes in the vibrational spectrum occur at 2.1 GPa. The 3200 cm⁻¹ vibrational mode splits into two peaks at 3190 and 3220 cm⁻¹, and an additional vibrational mode appears at 3255 cm⁻¹. The abrupt change in the spectrum indicates a phase transition at 2.1 GPa, consistent with the findings from the XRD

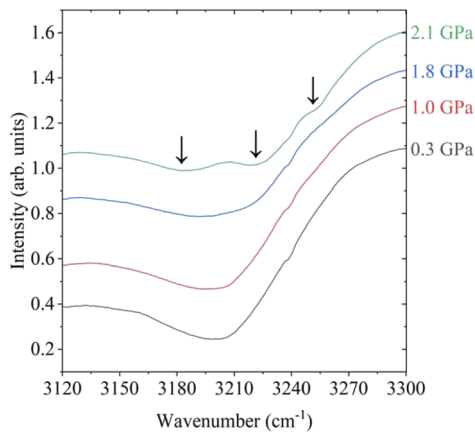


FIG. 4. Transmission spectra for β -ZnTe(en) $_{0.5}$ with mineral oil at four different pressures. The lower three pressures indicate that the sample is in the low-pressure phase. The appearance of IR peaks at 2.1 GPa, designated by arrows, indicates a phase transition.

measurements, where the new phase exhibits additional IR-active NH_2 stretching vibrational modes.

Figure 5 displays the C–H vibrational modes in the 2900–3025 cm^{-1} range for measurements performed with liquid nitrogen as a pressure-transmitting medium. At 1.9 GPa, two peaks are observed at 2920 and 2940 cm^{-1} , corresponding to CH_2 stretching modes.²⁷ Between 1.9 and 2.2 GPa, a distinct spectral change occurs: at 2.2 GPa, the two peaks merge into a single broad peak with maximum absorption at 2950 cm^{-1} . This is consistent with a phase transition between 1.9 and 2.2 GPa, verifying the conclusion made with XRD measurements and IR measurements performed with mineral oil.

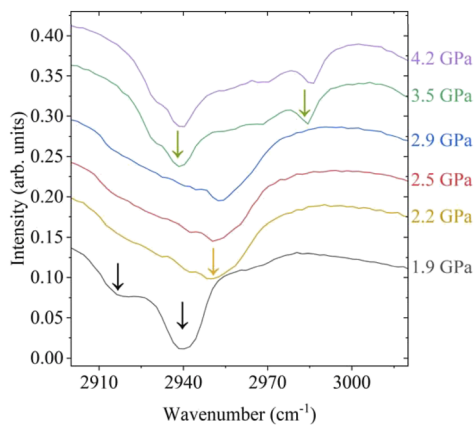


FIG. 5. Transmission spectra for β -ZnTe(en) $_{0.5}$ with liquid nitrogen at six different pressures. At 1.9 GPa, the sample is in the low-pressure phase. The change in vibrational modes at 2.2 GPa indicates a phase transition. The change in vibrational modes at 3.5 GPa indicates that the sample has undergone a second phase transition between 2.9 and 3.5 GPa. Arrows indicate IR peaks for each phase.

The spectra taken between 2.2 and 2.9 GPa show the same vibrational mode at 2950 cm^{-1} . The spectrum taken at 3.5 GPa indicates another change in the vibrational modes. In that spectrum and the following spectrum at 4.2 GPa, there are two peaks at 2935 and 2985 cm^{-1} . The change in CH_2 stretching vibrational modes indicates a second phase transition occurring between 2.9 and 3.5 GPa, consistent with findings from the XRD measurements that indicated a phase transition at 3.3 GPa.

CONCLUSIONS

In conclusion, this study provides evidence of pressure-induced phase transitions in β -ZnTe(en) $_{0.5}$ at 2.1 and 3.3 GPa. XRD measurements showed splittings in the (020) and (130) peaks, and FTIR spectroscopy further demonstrated changes in the vibrational modes at both phase transition pressures. These transitions occur at pressures significantly lower than the lowest reported phase change for pure ZnTe. Both phase transitions are characterized by substantial decreases in the b lattice parameter, attributed to the compression of the organic layer. Similar to In_2Se_3 , which also experiences phase transitions at relatively moderate pressures,^{10,30} multiple phases of ZnTe(en) $_{0.5}$ could potentially be utilized in memory devices.

Our findings indicate that the pressure response of ZnTe(en) $_{0.5}$ is highly anisotropic; specifically, the organic layer is very responsive to pressure changes. This anisotropy results in larger strain along the layer stacking direction (the b axis) than in the a direction for a given pressure. However, our experimental findings are at odds with previous calculations of the elastic constants.²⁶ In the future, elastic constant measurements using ultrasonic methods, along with first-principles calculations, may be beneficial in resolving this discrepancy.

SUPPLEMENTARY MATERIAL

See the [supplementary material](#) for XRD details, IR spectra taken for decreasing pressures, and strain calculations.

ACKNOWLEDGMENTS

The authors would like to acknowledge Brian Collins, Tanner Melody, and Zachary Heiden for their assistance with the XRD measurements. The work at Washington State University was supported by the U.S. Department of Energy, Office of Basic Energy Sciences, Division of Materials Science and Engineering under Award No. DE-FG02-07ER46386. The Xeuss XRD facility was supported by a grant from the MJ Murdock Charitable Trust. Work at UNC Charlotte was supported by ARO/Complex Dynamics and Systems Program under Grant No. W911NF-23-1-0215.

AUTHOR DECLARATIONS

Conflict of Interest

The authors have no conflicts to disclose.

Author Contributions

Julianne C. Miller: Formal analysis (equal); Investigation (equal); Methodology (equal); Writing – original draft (lead). **Yizhou Wang:** Investigation (supporting); Methodology (supporting). **Yong**

Zhang: Conceptualization (equal); Formal analysis (equal); Funding acquisition (equal); Investigation (equal); Writing – review & editing (equal). **Thomas A. Schmedake:** Investigation (supporting); Methodology (supporting). **Matthew D. McCluskey:** Conceptualization (equal); Data curation (equal); Formal analysis (equal); Funding acquisition (equal); Investigation (equal); Methodology (equal); Project administration (lead); Supervision (lead); Writing – review & editing (lead).

DATA AVAILABILITY

The data that support the findings of this study are available in the paper and its [supplementary material](#).

REFERENCES

- ¹M. Wright and A. Uddin, “Organic–inorganic hybrid solar cells: A comparative review,” *Sol. Energy Mater. Sol. Cells* **107**, 87–111 (2012).
- ²W. Liu, W. P. Lustig, and J. Li, “Luminescent inorganic-organic hybrid semiconductor materials for energy-saving lighting applications,” *EnergyChem* **1**(2), 100008 (2019).
- ³G. Kickelbick, *Hybrid Materials: Synthesis, Characterization, and Applications* (Wiley-VCH Verlag GmbH & Co. KGaA, New York, 2007).
- ⁴T. Ye, M. Kocherga, Y.-Y. Sun, A. Nesmelov, F. Zhang, W. Oh, X.-Y. Huang, J. Li, D. Beasock, D. S. Jones, T. A. Schmedake, and Y. Zhang, “II–VI organic–inorganic hybrid nanostructures with greatly enhanced optoelectronic properties, perfectly ordered structures, and shelf stability of over 15 years,” *ACS Nano* **15**(6), 10565–10576 (2021).
- ⁵X. Huang, J. Li, Y. Zhang, and A. Mascarenhas, “From 1D chain to 3D network: Tuning hybrid II–VI nanostructures and their optical properties,” *J. Am. Chem. Soc.* **125**(23), 7049–7055 (2003).
- ⁶B. Fluegel, Y. Zhang, A. Mascarenhas, X. Huang, and J. Li, “Electronic properties of hybrid organic–inorganic semiconductors,” *Phys. Rev. B* **70**(20), 205308 (2004).
- ⁷Y. Zhang, “II–VI based organic-inorganic hybrid structures: Brief review and perspective,” *J. Lumin.* **248**, 118936 (2022).
- ⁸A. Poglitsch and D. Weber, “Dynamic disorder in methylammoniumtrihalogenoplumbates (II) observed by millimeter-wave spectroscopy,” *J. Chem. Phys.* **87**(11), 6373–6378 (1987).
- ⁹R. J. Elliott, J. A. Krumhansl, and P. L. Leath, “The theory and properties of randomly disordered crystals and related physical systems,” *Rev. Mod. Phys.* **46**(3), 465–543 (1974).
- ¹⁰A. M. Rasmussen, S. T. Teklemichael, E. Mafi, Y. Gu, and M. D. McCluskey, “Pressure-induced phase transformation of In_2Se_3 ,” *Appl. Phys. Lett.* **102**(6), 062105 (2013).
- ¹¹B. Gupta, J. Bhalavi, S. Sharma, and A. Bisen, “Phase change materials in solar energy applications: A review,” *Mater. Today: Proc.* **46**, 5550–5554 (2021).
- ¹²X. Huang, J. Li, and H. Fu, “The first covalent organic–inorganic networks of hybrid chalcogenides: Structures that may lead to a new type of quantum wells,” *J. Am. Chem. Soc.* **122**(36), 8789–8790 (2000).
- ¹³M. G. Giorgini, M. R. Pelletti, G. Paliani, and R. S. Cataliotti, “Vibrational spectra and assignments of ethylene-diamine and its deuterated derivatives,” *J. Raman Spectrosc.* **14**(1), 16–21 (1983).
- ¹⁴T. Suski and T. Paul, *High Pressure in Semiconductor Physics I* (Academic Press, 1998).
- ¹⁵G. Shen, Y. Wang, A. Dewaele, C. Wu, D. E. Fratanduono, J. Eggert, S. Klotz, K. F. Dziubek, P. Loubeyre, O. V. Fat’yanov, P. D. Asimow, T. Mashimo, and R. M. M. Wentzcovitch, “Toward an international practical pressure scale: A proposal for an IPPS ruby gauge (IPPS-Ruby2020),” *High Pressure Res.* **40**(3), 299–314 (2020).
- ¹⁶L. M. Barmore, J. Jesenovc, J. S. McCloy, and M. D. McCluskey, “Photoluminescence of Cr^{3+} in $\beta\text{-Ga}_2\text{O}_3$ and $(\text{Al}_{0.1}\text{Ga}_{0.9})_2\text{O}_3$ under pressure,” *J. Appl. Phys.* **133**(17), 175703 (2023).
- ¹⁷A. Jayaraman, “Diamond anvil cell and high-pressure physical investigations,” *Rev. Mod. Phys.* **55**(1), 65–108 (1983).
- ¹⁸R. J. Angel, M. Bujak, J. Zhao, G. D. Gatta, and S. D. Jacobsen, “Effective hydrostatic limits of pressure media for high-pressure crystallographic studies,” *J. Appl. Crystallogr.* **40**(1), 26–32 (2007).
- ¹⁹S. Klotz, J.-C. Chervin, P. Munsch, and G. Le Marchand, “Hydrostatic limits of 11 pressure transmitting media,” *J. Phys. D: Appl. Phys.* **42**(7), 075413 (2009).
- ²⁰G. Ning and R. L. Flemming, “Rietveld refinement of LaB_6 : Data from μXRD ,” *J. Appl. Crystallogr.* **38**(5), 757–759 (2005).
- ²¹A. Hybl and R. E. Marsh, “Structure factor and least-squares calculations for orthorhombic systems with anisotropic vibrations,” *Acta Crystallogr.* **14**(10), 1046–1051 (1961).
- ²²P. Indelicato and E. Lindroth, “Relativistic effects, correlation, and QED corrections on $K\alpha$ transitions in medium to very heavy atoms,” *Phys. Rev. A* **46**(5), 2426–2436 (1992).
- ²³J. A. Bearden, “X-ray wavelengths,” *Rev. Mod. Phys.* **39**(1), 78 (1967).
- ²⁴C.-Y. Moon, G. M. Dalpian, Y. Zhang, S.-H. Wei, X.-Y. Huang, and J. Li, “Study of phase selectivity of organic–inorganic hybrid semiconductors,” *Chem. Mater.* **18**(12), 2805–2809 (2006).
- ²⁵P. Karil, N. Karma, H. S. Dager, and N. Kaurav, “Study of structural phase transition and elastic properties of ZnTe semiconducting compound under high pressure,” *Mater. Today: Proc.* **54**, 782–785 (2022).
- ²⁶X. Qian, X. Gu, and R. Yang, “Anisotropic thermal transport in organic–inorganic hybrid crystal $\beta\text{-ZnTe}(\text{en})_{0.5}$,” *J. Phys. Chem. C* **119**(51), 28300–28308 (2015).
- ²⁷A. Sabatini and S. Califano, “Infra-red spectra in polarized light of ethylenediamine and ethylenediamine– d_4 ,” *Spectrochim. Acta* **16**(6), 677–688 (1960).
- ²⁸L. Segal and F. V. Eggerton, “Infrared spectra of ethylenediamine and the dimethylethylenediamines,” *Appl. Spectrosc.* **15**(4), 116–117 (1961).
- ²⁹J. Hudecová, V. Profant, P. Novotná, V. Baumruk, M. Urbanová, and P. Bouř, “CH stretching region: Computational modeling of vibrational optical activity,” *J. Chem. Theory Comput.* **9**(7), 3096–3108 (2013).
- ³⁰A. M. Rasmussen, E. Mafi, W. Zhu, Y. Gu, and M. D. McCluskey, “High pressure γ -to- β phase transition in bulk and nanocrystalline In_2Se_3 ,” *High Pressure Res.* **36**(4), 549–556 (2016).